Mathematical model for contemplative amoeboid locomotion

Kei-Ichi Ueda
Research Institute for Mathematical Sciences, Kyoto University, Kyoto 606-8502, Japan

Seiji Takagi, Yasumasa Nishiura, and Toshiyuki Nakagaki*
Research Institute for Electronic Science, Hokkaido University, Sapporo 001-0020, Japan

(Received 31 March 2010; revised manuscript received 9 November 2010; published 28 February 2011)

It has recently been reported that even single-celled organisms appear to be "indecisive" or "contemplative" when confronted with an obstacle. When the amoeboid organism *Physarum* plasmodium encounters the chemical repellent quinine during migration along a narrow agar lane, it stops for a period of time (typically several hours) and then suddenly begins to move again. When movement resumes, three distinct types of behavior are observed: The plasmodium continues forward, turns back, or migrates in both directions simultaneously. Here, we develop a continuum mathematical model of the cell dynamics of contemplative amoeboid movement. Our model incorporates the dynamics of the mass flow of the protoplasmic sol, in relation to the generation of pressure based on the autocatalytic kinetics of pseudopod formation and retraction (mainly, sol-gel conversion accompanying actin-myosin dynamics). The biological justification of the model is tested by comparing with experimentally measured spatiotemporal profiles of the cell thickness. The experimentally observed types of behavior are reproduced in simulations based on our model, and the core logic of the modeled behavior is clarified by means of nonlinear dynamics. An on-off transition between the refractory and activated states of the chemical reactivity that takes place at the leading edge of the plasmodium plays a key role in the emergence of contemplative behavior.

DOI: 10.1103/PhysRevE.83.021916 PACS number(s): 87.17.Jj, 87.17.Aa, 05.40.−a

I. INTRODUCTION

It is remarkable that even single-celled organisms can exhibit complex behavior [1]. Consequently, the possible existence of primitive psychic life at the level of the cell has been suggested. One elegant example was reported three years ago: The giant amoeba of *Physarum* plasmodium can demonstrate behavior that is "indecisive" or "contemplative" in nature [2]. When this slime mold encountered low concentrations of the toxic chemical quinine, it temporarily stopped migrating. The period of time for which migration stopped was unpredictable and varied case by case. Nevertheless, after several hours the plasmodium suddenly began to migrate again, in one of three different ways: penetration through the toxic zone, rebounding back from the toxic zone, and the intermediate case in which the migration front split into both penetration and rebound parts. This phenomenon represents the selection of behavior after different periods of quiescence that depend on the individual organism.

Interestingly, a phenomenological mathematical model for understanding the mechanism of this contemplative behavior was also proposed in Ref. [2]. The model is, however, too abstract to test the correspondence of the model variables and parameters with real phenomena, although the core mathematical mechanism is plausible and probably valid.

In this article, we try to develop a more realistic model that incorporates the dynamics of the mass flow of protoplasmic sol and reproduces the three different types of behavior. We keep the core part of the dynamics described in the previous model. Our model is constructed such that its biological justification can be studied; we examine it in detail from a cytological point of view. The purpose of the modeling is to construct a reliable interface between the complex biochemical processes of directed cellular locomotion and the core mechanism of nonlinear dynamics, which is relatively simple.

We test the biological justification of our model by experimentally measuring cell thickness profiles for the three different types of contemplative behavior. By means of numerical simulations based on the proposed model, these measurements allow us to study the deformation of a realistic cell shape that occurs with the mass flow of the protoplasm.

The core dynamics of the previously proposed model has thus far been considered only from a mathematical point of view. The importance of the saddle-type nature of the transient dynamics in dissipative systems has previously been emphasized [3–6]. By carrying out numerical simulations using our proposed model, we show that a transition between the activated and refractory states of chemical reactivity at the leading edge of the plasmodium, which is regulated by the protoplasmic sol, is essential to explain the observed avoidance of the toxic region and the contemplative behavior.

This paper is organized as follows. First, we present a new experimental study of the spatiotemporal profile of the cell thickness for each type of contemplative behavior exhibited by *Physarum* plasmodium. Second, we propose a more realistic model to explain this behavior, based on the conventional model proposed in Ref. [2]. Finally, the mathematical essence of the dynamical behavior is clarified and the biological significance of the contemplative behavior is discussed within the context of the mathematics of nonlinear dynamics.

*Present address: Department of Complex and Intelligent Systems, Faculty of Systems Information Science, Future University Hakodate, Hakodate 041-8655, Japan; JST, CREST, Chiyoda ku Tokyo 102-0075, Japan.

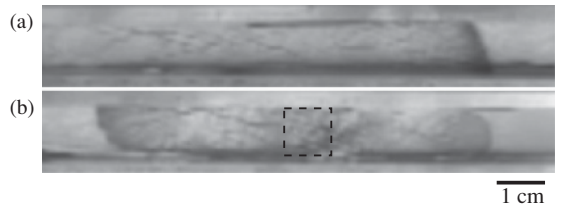

FIG. 1. Photographs of plasmodia migrating down an agar lane. (a) Plasmodium migrating under homogeneous conditions. (b) Plasmodium splitting into two fronts under inhomogeneous conditions [see Fig. 3(b) for details]. The placement of quinine on the agar plate is indicated by the dotted square.

II. EXPERIMENTAL STUDY

A. Organism and preparation

The plasmodium of *Physarum polycephalum* (strain HU195 × HU200) was fed oat flakes (Quaker Oats Co.) on 1% agar gel (Wako Pure Chemicals Inc.) at 25 °C in the dark. In this study, we performed two types of experiments. First, we investigated the locomotion activity of the leading edge of the plasmodium. Second, we examined the avoidance behavior exhibited by the *Physarum* plasmodium in a limited space. In all experiments, a fixed amount (100 mg) of the leading edge of a large plasmodium in a culture trough (25 cm × 35 cm) was cut off and placed at the end of a narrow agar lane (1.5%), which was 1 cm in width and 30 cm in length. The plasmodium then began to migrate directly toward the other end of the lane over a period of 30–60 min [for example, see Fig. 1(a)]. The entire organism, except for the frontal tip, showed coherent rhythmic contraction with a period of ∼2 min.

The experiments were carried out at 25 °C in the dark. The movement of the plasmodia was observed as described previously [2]. The plasmodia were illuminated from below using an infrared light source (λ ∼ 950 nm), and observed from above using a charge-coupled device (CCD) camera with a resolution of 640 × 480 pixels, in 8-bit grayscale. Images were stored directly on a personal computer at intervals of 6 s. The thickness of the plasmodium was estimated according to the Beer-Lambert law: $h \sim -\log I/I_0$, where h is the thickness, and I and I_0 are the transmitted and incident light intensities, respectively. Calibration was performed by placing the plasmodium between an agar plate and a cover glass with a small tilt angle.

B. Locomotion of frontal tip separated from main body

The plasmodium migrating down the lane was separated into a frontal tip and a main body using a knife (feather surgical blade #10), as shown in Fig. 2. After removal of the main body, only the frontal tip remained in the lane (at about 33 min in Fig. 2). Nevertheless, the frontal tip continued to migrate for 10 min at almost the same velocity as before amputation. The extension gradually slowed as the frontal tip became thinner (at approximately 50 min). Finally, migration stopped. This result suggests that migration of the front of the plasmodium is driven by a process localized at the tip, but that a supply of protoplasm from the rear part is necessary for maintaining locomotion over longer periods of time.

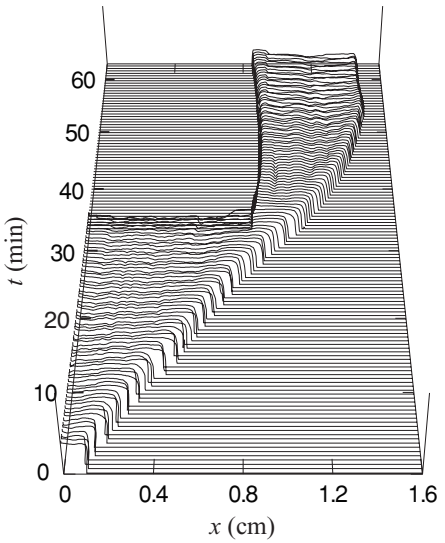

FIG. 2. Effect of amputation of the frontal tip. Thickness profiles (arbitrary units) as a function of position along the agar lane x are plotted. The origin of x and t is defined arbitrarily. Amputation was performed at about 8 h after preparation. A plasmodium of ∼9 cm in length migrated toward the right; after 33 min a cut was made at 2.5 mm from the front and the main body was removed.

C. Behavior upon encountering quinine

We next studied the behavior of the plasmodium when it encountered a repellent, quinine. The repellent region, of fixed length 10 mm, consisted of a block of agar gel containing quinine embedded in the middle of the lane. The plasmodium was forced to face the repellent due to the limited space in the lane, as shown in Fig. 1(b). The effects of quinine concentrations of 4, 6, and 8 mM were examined.

The plasmodia exhibited three distinct types of cell behavior depending on the concentration of quinine, as shown by the time traces of the thickness profiles in Fig. 3. In all three cases, the plasmodium stopped migrating at the repellent region for a period of several hours; the duration differed between experiments. The plasmodium then suddenly began to move again, in a manner that depended on the quinine concentration. When the concentration was low (4 mM), the plasmodium migrated through the repellent region after stopping for about 6 h [Fig. 3(a)]. When the concentration was high (8 mM), the plasmodium reversed direction after stopping for about 15 h [Fig. 3(c)]. At the intermediate quinine concentration (6 mM), the plasmodium exhibited both types of behavior simultaneously; that is, part of the plasmodium moved through the repellent region and the other part reversed direction, after stopping for about 8 h [Fig. 3(b); see also Fig. 1(b)]. In other words, the plasmodium split into two fronts migrating in opposite directions.

Here, the following points should be noted. First, the splitting behavior was not exclusively observed at the intermediate repellent concentration; penetration and rebound behavior were also observed on a case-by-case basis. Second, the period of stopping differed on a case-by-case basis even under identical conditions.

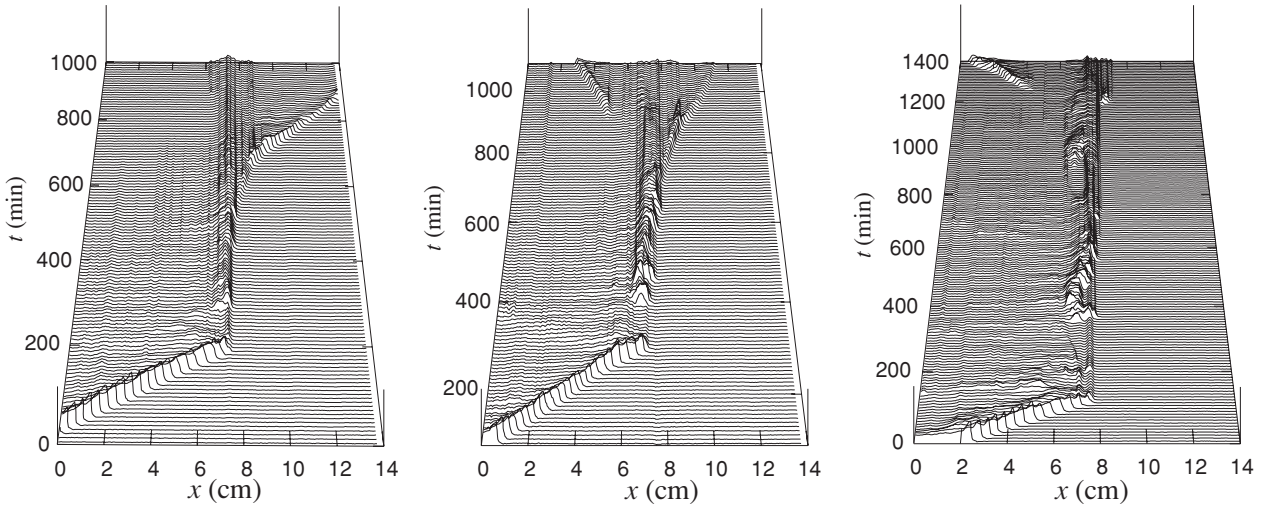

FIG. 3. Three different types of behavior exhibited by *Physarum* plasmodia upon encountering the repellent. Thickness profiles are plotted in the same manner as in Fig. 2. The plasmodia exhibited (a) penetration, (b) splitting, and (c) rebound behavior at quinine concentrations of 4, 6, and 8 mM, respectively.

III. MODEL

Let us now derive a model equation describing the cell propagation in a one-dimensional domain. A schematic picture of the cell cross section along the axis of migration is shown in Fig. 4. The organism consists of an endoplasmic sol layer and an ectoplasmic gel layer. The gel is composed of actomyosin filaments. The sol layer is covered by the gel layer. The streaming of protoplasmic sol is driven by a pressure gradient generated by contraction of the actomyosin filaments in the gel layer. Thus, we use a two-layer model.

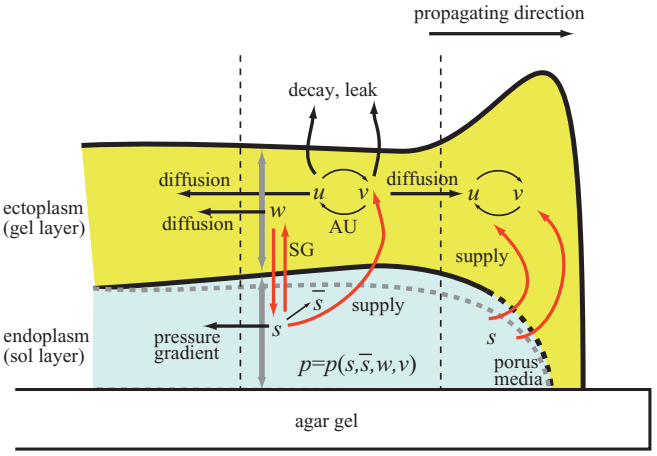

FIG. 4. (Color online) Schematic illustration of the proposed model, showing a cross section of the organism along the axis of propagation. Chemical reactions that generate the leading edge can be considered as autocatalytic reactions (AU) between u and v. The thicknesses of the gel and sol layers are w and $\bar{s}$, respectively. The thickness of the gel changes with time due to sol-gel transformation (SG). The pressure of the sol is described by a function of s, $\bar{s}$, w, and v. The solation factors and regulation factors are supplied by the sol. Because the edge of the organism is a porous medium, the supply rates of u and v from the sol at the leading edge are taken to be larger than those in the main body.

In essence, the locomotion of *Physarum polycephalum* is established by the following three steps (Fig. 5). (i) In order to generate a leading edge, the organism decreases the stiffness of the gel at the boundary edge by means of chemical reactions that take place there. As the stiffness of the gel at the frontal part of the plasmodium decreases, the pressure of the sol at the frontal part decreases concomitantly. (ii) The sol is transported from the rear part to the leading edge due to the pressure gradient generated by process (i). (iii) The sol at the leading edge, transported from the rear part by process (ii), is transformed into gel. Thus, a fresh gel layer is newly generated at the frontal part. It is essential to describe the dynamics involved in each process (i)–(iii): the dynamics of the chemical reaction that generates a spatial pressure gradient in the sol layer, the protoplasmic sol streaming, and the sol-gel transformation.

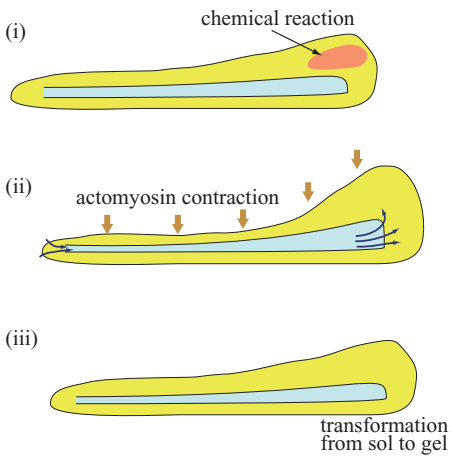

FIG. 5. (Color online) Schematic representation of cell locomotion. See the main text for explanation.

Modeling studies of the dynamics of the intracellular protoplasmic sol have been reported in Refs. [7–9], and a dimensionless model equation has been proposed by Kobayashi *et al.* [8]. Our model is based on the model derived in Ref. [8], but it uses a more detailed setting in order to formulate an equation for the protoplasmic sol streaming, as described in Sec. III A. In Secs. III B and III C, the dynamics of sol-gel transformations and chemical reactions in the gel layer are incorporated into the model derived in Sec. III A.

A. Dynamics of protoplasmic sol streaming: Conventional model

The mass of sol is described by $s(x,t)$, where $x \in [0,L]$ and $t \geqslant 0$ are the variables representing space and time, respectively. The flow of sol is governed by Darcy's law:

$$s_t = (sMp_x)_x, \tag{1}$$

where M is the mobility coefficient. The organism has a basal thickness of the sol layer, $s_b(x,t)$, like the natural length of a Hookian spring. We assume that the dynamics of the pressure of the sol, $p(x,t)$, is governed by the following equation:

$$p = \beta f\left(\frac{s - s_b}{\bar{s}}\right), \tag{2}$$

where $\bar{s} = \bar{s}(x,t)$ is the thickness of the sol layer. We assume that the elastic force is determined by the displacement of contraction from the basal thickness s_b per unit thickness. It has been experimentally observed that $\bar{s}(x,\cdot)$ increases as the amount of sol at position x increases. Therefore, we assume that $\bar{s}$ is determined by the quantity of s averaged over time $\tau_{\bar{s}}$. The dynamics of $\bar{s}$ is described as follows:

$$\tau_{\bar{s}}\bar{s}_t = D_{\bar{s}}\bar{s}_{xx} + s - \bar{s}, \tag{3}$$

where $D_{\bar{s}}$ is a diffusion coefficient. Equation (3) makes $\bar{s}$ a weighted running average of s over a time scale of order $\tau_{\bar{s}}$. The diffusion term in (3) is introduced for a smoothing effect, which comes from the elastic property of protoplasm (see Ref. [8] for details).

We assume that s_b varies periodically in time, which corresponds to actomyosin contraction. Here we assume that the periodic oscillation can be simply described by a sine function. In addition, because the amplitude of the actomyosin contraction increases as the actomyosin bundles mature, the amplitude of the oscillation should be a function of the thickness of the gel, $w(x,t)$. Thus, we assume that $s_b(x,t)$ is described as follows:

$$s_b = \bar{s} - w[a_0 + a_1 \sin(\omega t)], \tag{4}$$

where ω is the angular velocity. For simplicity, we assume that the phase of the oscillation of s_b is independent of x.

Because the actomyosin system produces a stronger force in the contraction phase than in the relaxation phase, the function f is given by the following formulation (see Fig. 6):

$$f(\xi) = \begin{cases} \xi & \text{for} \quad \xi > 0, \\ \xi(1 - \xi/c)^{-1} & \text{otherwise.} \end{cases} \tag{5}$$

The parameter β represents the pressure when s is increased from $\bar{s}_b$ by $\bar{s}$, because $f(1) = 1$. That is, β corresponds to the stiffness of the gel.

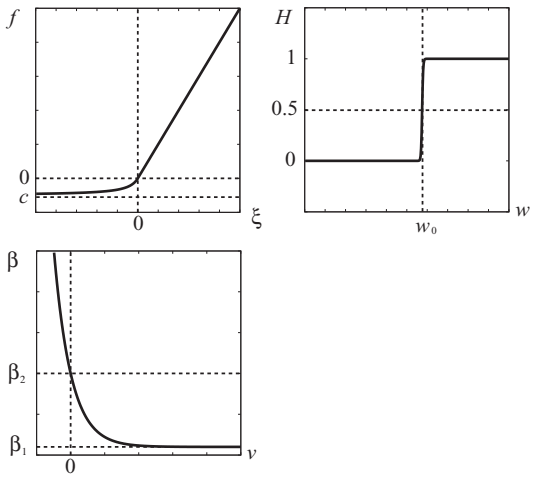

FIG. 6. Profiles of functions $f(\xi)$, $H(w)$, and $\beta(v)$.

B. Sol-gel transformation

Because the transformations from gel to sol and from sol to gel take place bidirectionally in the organism, we assume that the thickness of the gel layer tends to approach an equilibrium value that depends on the amount of sol (i.e., $s/w \to \gamma_2$ as $t \to \infty$, where γ_2 is a positive constant). Thus, the dynamics of w is described as follows:

$$w_t = D_w w_{xx} + \gamma_1(s - \gamma_2 w), \tag{6}$$

where D_w is a diffusion coefficient. Because the total mass of the organism is conserved, $s + w$ is conserved over the entire space. Thus, the equation for s is modified with respect to (1), and we obtain the following:

$$s_t = (sMp_x)_x + \gamma_1(\gamma_2 w - s). \tag{7}$$

C. Localized concentration pattern of solation factors

It is experimentally observed that the gel at the frontal part of the plasmodium is softer than that in the rear part. The stiffness of the gel depends on the aggregation state of the actomyosin filaments. For example, the strength of the gel increases as the bundles thicken, the cross links become denser, and the arrangement of the bundles becomes more regular. The gel state can be converted to the sol state in response to solation factors.

It has also been experimentally observed that when the leading edge migrates, structures containing high concentrations of adenosine triphosphate (ATP) [10,11], Ca^{2+} [12,13], and Fragmin [14,15] are present in the gel layer at the leading edge. The migration stops when these localized concentration patterns disappear, indicating that such patterns are essential for the cell to maintain migration. Experimental studies have suggested that the chemicals involved are solation factors (e.g., Fragmin [14], Ca^{2+} [13,16,17], and ATP [18]). The chemical reactions that control the stiffness of the gel are then responsible for generating the leading edge. These considerations imply that the localized concentration patterns are generated by the diffusion of solation factors and regulation factors of the solation factors, and by chemical reactions among them (i.e., a reaction-diffusion process).

Let us now derive model equations for the reaction-diffusion process that takes place in the gel layer. We first propose a model equation for the situation in which the organism is uniformly spread throughout the space available. The reaction-diffusion process is described by

$$\begin{aligned} \tau u_t &= (D_u u_x)_x - F(u,v) - r_u u + \sigma_u(u_0 - u), \\ \tau v_t &= (D_v v_x)_x + F(u,v) - r_v v + \sigma_v(v_0 - v), \end{aligned} \tag{8}$$

where v and u represent the concentrations of the solation factors and of the regulation factors of the solation factors, respectively. The first term on the right-hand side of Eqs. (8) represents the diffusion processes for u and v. The second term represents autocatalytic chemical reactions between the solation factors and the regulation factors. The third term represents decay and leakage processes involving these chemicals. The fourth term represents the supply rate of the chemicals from the sol layer, where u_0 and v_0 are the concentrations of the regulation factors and solation factors in the sol layer. Because the diffusion rate of chemical substances in the sol layer is relatively large compared to that in the gel layer, we simply take u_0 and v_0 to be constant values.

We assume that the autocatalytic chemical reactions are described by Hill's law, which is a typical model used to describe such reactions in biochemical processes:

$$F(u,v) = \frac{uv^2}{k_1 + k_2 v^2}, \tag{9}$$

where k_1 and k_2 are positive constants.

The chemical reaction network in the organism is complex. It has been found that many chemicals including H^+, Ca^{2+}, K^+, ATP, and adenosine diphosphate (ADP) are involved in the reaction network [10,12,18–20]. Details of these chemical reactions are currently unclear. Therefore, we adopt a simple reaction term (9) to describe the fundamental dynamics of the reactions. However, this does not mean that the reactions are limited to the form described by (9). For example, the behavior shown in Fig. 3 can be qualitatively reproduced by $F(u,v) = uv^3/(k_1 + k_2 v^3)$ and $F(u,v) = u^2v^2/(k_1 + k_2 v^2)$.

During locomotion, gel is generated in the anterior part of the organism and is transformed into sol in the posterior part. Such a process may induce topological changes of the organism; for example, the organism can divide itself into two parts by splitting (see Fig. 3). Such topological changes require us to define the region of existence of the organism. In order to describe the existence region of the gel, we employ the phase field function

$$H(w) = \{1 + \tanh[\gamma(w - w_0)]\}/2, \tag{10}$$

where w_0 is a small constant that corresponds to the threshold thickness of the organism. The boundary of the organism is represented by the sharp layer of the function. The position of the transition layer is taken to be the point at which $w = w_0$; $H \approx 1$ for $w > w_0 + \delta$ (δ is a small positive constant) and $H(w) \approx 0$ for $w < w_0 - \delta$ when γ is sufficiently large (Fig. 6). Here, we fix $\gamma = 100$. For convenience, we refer to the region $\{x|H(w(x,\cdot)) \in [0.9,1.0]\}$ as the interior part, the region $\{x|H(w(x,\cdot)) \in [0.1,0.9)\}$ as the boundary edge, and the region $\{x|H(w(x,\cdot)) \in [0.0,0.1)\}$ as the exterior part.

We assume that the diffusion process obeys the first term of (8) in the interior part (D_u and D_v are constants), and that the chemicals do not diffuse in the exterior part ($D_u = D_v = 0$). Using H, we formulate the diffusion coefficients as continuous functions of w:

$$\begin{aligned} D_u(w) &= H(w)\bar{D}_u, \\ D_v(w) &= H(w)\bar{D}_v, \end{aligned} \tag{11}$$

where $\bar{D}_u$ and $\bar{D}_v$ are the diffusion coefficients in the interior part.

We assume that the autocatalytic chemical reactions occur in a region where gel exists. Therefore, we replace $F(u,v)$ in (8) by $H(w)F(u,v)$.

Experimental observations have shown that the properties of the structure of the organism at the boundary edge are different from those in the interior part. In particular, the following have been reported:

(i) Slime-containing vesicles, which are transported from the posterior part to the anterior part in the sol layer, are exposed at the boundary edge and reconstruction of the membrane occurs [21].

(ii) The leading edge is a porous medium, thus the tube structure at the leading edge is not mature.

The event in (i) perhaps increases the concentrations of solation factors and regulation factors temporarily. Given the observation in (ii), it is reasonable to assume that the supply rates of u and v at the boundary edge (σ_u and σ_v, respectively) are higher than in the interior part, because the porous medium enables the sol to easily permeate into the gel layer. In addition, the supply rates should be expressed as functions of s, because they should be 0 at the place where $s = 0$. We assume that σ_u and σ_v take the following forms:

$$\sigma_* = \sigma_*(s) = \begin{cases} \sigma_*^i g(s) & \text{in the interiorpart}, \\ \sigma_*^b g(s) & \text{at the boundaryedge}, \\ 0 & \text{in the exteriorpart}. \end{cases} \tag{12}$$

Here, $* = \{u,v\}$; σ_*^i and σ_*^b are positive constants. The quantity $g(s)$ is a monotonically increasing function of s:

$$g(s) = \begin{cases} \frac{s}{s_0} & \text{for } s < s_0, \\ \frac{1}{s_0}\left(\frac{s - s_0}{1 + k_3(s - s_0)}\right) + 1 & \text{for } s \geqslant s_0, \end{cases} \tag{13}$$

where k_3 is a positive constant. We note that $g(s)$ satisfies $g(0) = 0$ and $g(+\infty) = 1 + 1/s_0 k_3$. As a result, Eqs. (8) are modified as follows:

$$\begin{aligned} \tau u_t &= [D_u(w)u_x]_x - H(w)F(u,v) - r_u u + \sigma_u(s)(u_0 - u), \\ \tau v_t &= [D_v(w)v_x]_x + H(w)F(u,v) - r_v v + \sigma_v(s)(v_0 - v). \end{aligned} \tag{14}$$

Finally, we describe the stiffness of the gel as a function of the solation factors, v. We take β in (2) to be a monotonically decreasing function of v as follows:

$$\beta(v) = \beta_1 + (\beta_2 - \beta_1)\exp(-\beta_3 v), \tag{15}$$

where β_1, β_2, and β_3 are positive constants.

IV. RESULTS

A. Locomotion in homogeneous media

We first describe the mechanism by which one-way propagation of the organism occurs in homogeneous media. We will then reproduce the contemplative behavior observed when the organism encounters a chemical repellent.

In our numerical simulations, the Neumann boundary condition was used. The values of the parameters used in the numerical simulations are set to $L = 6$, $M = 0.2$, $\tau_{\bar{s}} = 0.2$, $D_{\bar{s}} = 1.0$, $c = 0.1$, $a_0 = 0.35$, $a_1 = 0.45$, $\omega = 2\pi/1.08$, $D_w = 0.01$, $\gamma_1 = 10.0$, $\gamma_2 = 1.0$, $k_1 = 10.0$, $k_2 = 3.0$, $\gamma = 100$, $w_0 = 0.0175$, $\bar{D}_u = 1.0 \times 10^{-5}$, $\bar{D}_v = 1.0 \times 10^{-4}$, $\sigma_u^i = 0.0$, $\sigma_u^b = 0.15$, $\sigma_v^i = 0.015$, $\sigma_v^b = 0.02$, $u_0 = 10.0$, $v_0 = 1.0$, $k_3 = 10.0$, $s_0 = 0.02$, $r_u = 0.01$, $r_v = 0.23$, $\beta_1 = 0.1$, $\beta_2 = 5.0$, and $\beta_3 = 3.0$.

As an initial datum, a localized sol was placed near the left-hand boundary wall. The total sum of $s(x,0)$ over $x \in [0,L]$ is 5.0. We take r_v as a control parameter and observe the migration behavior. When r_v is sufficiently large, the system described by (14) enters the refractory state and the organism does not begin to migrate. If a smaller value of r_v is taken, the system enters an activated state and a localized concentration pattern of v is observed near the right-hand edge of the organism [Fig. 7(a)]. Furthermore, a localized pattern of s is simultaneously generated. The spatial profile of s is similar to that of v.

At the leading edge, a type of positive feedback between the activity expressed by (14) and the sol transportation is observed. Because more solation factors (v) are supplied as s is increased, the activity of the system described by (14) is sustained near the leading edge. The motility force becomes higher in the posterior part than in the anterior part because the pressure in the latter decreases due to the activity of the system. Thus, the position of the entire organism moves toward the leading edge and the localized concentration patterns of v and s are sustained. This positive feedback loop results in the observation of a one-way propagating localized concentration pattern. Such migration dynamics can be observed for $r_v \leqslant 0.27$.

B. Reproduction of locomotion behavior after amputation

It was found experimentally that the leading edge of the organism propagated for a certain time after amputation of the main body. This indicates that the leading edge can propagate regardless of the oscillatory contractile force generated in the main body. In our numerical simulations, amputation was expressed by abruptly setting the variables u, v, and s to 0 for $x \leqslant x_0$ at $t = t_0$, where x_0 is the amputation position. It was observed experimentally that the contraction oscillation disappears for a certain period of time after amputation; thus, we set the parameters a_0 and a_1 in (4) to 0 for $t \geqslant t_0$ and $x \leqslant x_0$. We set $x_0 = 1.44$ and $t_0 = 36$.

As shown in Fig. 7(b), the propagation of the leading edge continues for a certain time after amputation because the activity of the autocatalytic reaction described in (14) can be sustained as long as a sufficient quantity of s remains at the leading edge. However, the amount of s at the leading edge gradually decreases after amputation, and propagation finally stops [Fig. 7(b)]. Such locomotion behavior is in good agreement with the experimental results presented in Fig. 3. The numerical results shown in Figs. 7(a) and 7(b) indicate that, in order to maintain the migrating process, enough amount of the sol must be transported to the leading edge.

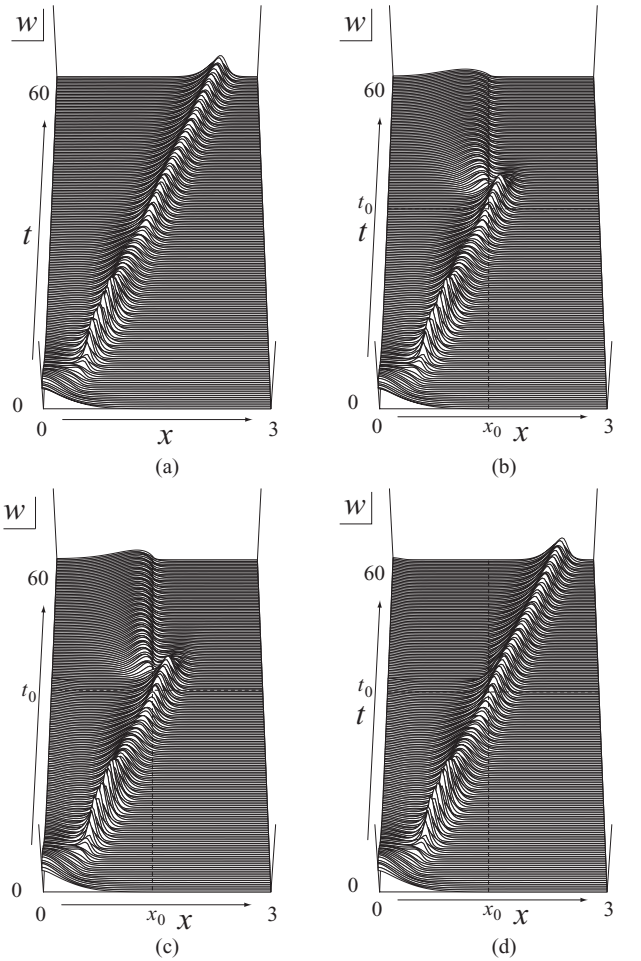

FIG. 7. (a) Migration in homogeneous media. (b) Behavior after amputation. The frontal tip is divided from the main body at $t = t_0 = 36$. For $x \leqslant x_0 = 1.44$, the variables u, v, and s were abruptly set to 0 at $t = t_0$, and the parameters a_0 and a_1 were set to 0 for $t \geqslant t_0$. (c) [(d)] The term $\sin(\omega t)$ in (4) is changed to -1 [$+1$] for $t \geqslant t_0$ and $x \leqslant x_0$.

We remark on the effect of the oscillatory motion on the locomotion. Suppose that the oscillatory phase $\theta = \omega t$ is fixed at the relaxation phase (i.e., $\theta \equiv -\pi/2$) for $t \geqslant t_0$ and $x \leqslant x_0$, but no abrupt changes for a_0, a_1, u, v, and s are supposed. Then the migrating process stops at finite time [Fig. 7(c)] since the pressure at the main body is low. On the other hand, if the oscillatory phase is fixed at the contraction phase (i.e., $\theta \equiv \pi/2$) for $t \geqslant t_0$ and $x \leqslant x_0$, the migrating process can be maintained after amputation [Fig. 7(d)]. Although the oscillatory motion, which is observed in the actual organism, seems indispensable to realize the shuttle streaming of sol and the locomotion in one direction, more careful numerical and experimental studies are needed to conclude that the oscillatory motion is a necessary condition for the migrating process in view of the numerical results in Fig. 7.

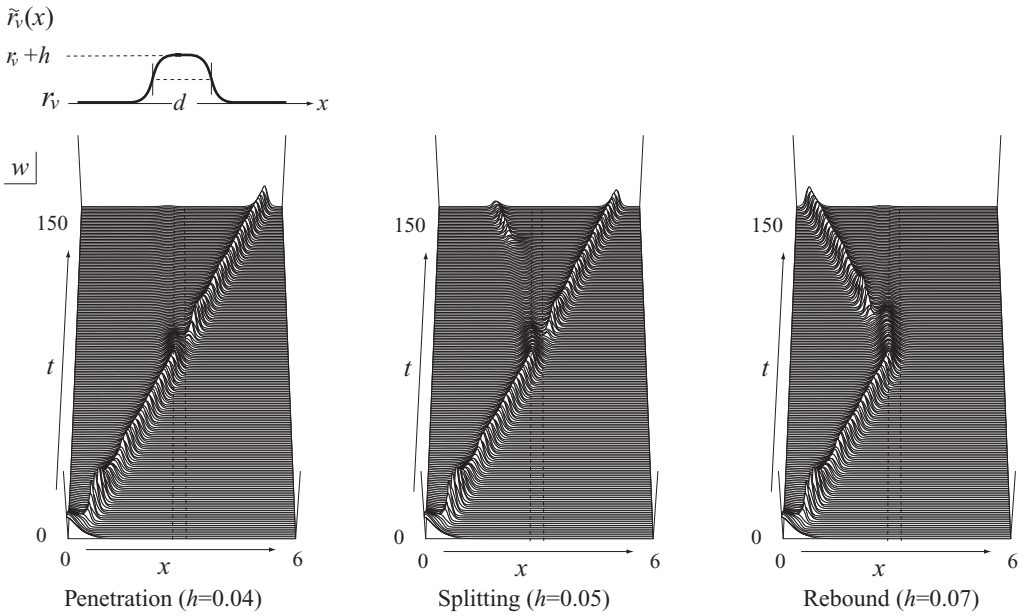

FIG. 8. Three types of response of the leading edge to encountering a repellent area. The dashed square indicates the repellent area.

C. Reproduction of responses to chemical repellent

In the experimental results shown in Fig. 3, the migration of the plasmodium suddenly decreases when the leading edge encounters a chemical repellent, and the organism stops migrating for a certain time. Such a change in activity can be reproduced in our simulations by abruptly and locally changing parameters in the system described by (14). One possible parameter that has a large influence on the activity of the frontal edge is the removal rate of the solation factors, r_v. We express the presence of the chemical repellent by taking r_v to be a function of x; specifically, we replace r_v by $\tilde{r}_v$, which is a function of x (Fig. 8):

$$\tilde{r}_v(x) = r_v + h\left\{\frac{1}{1+e^{\gamma_3[(x-L/2)-d/2]}} + \frac{1}{1+e^{-\gamma_3[(x-L/2)+d/2]}} - 1\right\},$$

where d is the width of the region containing a chemical repellent of concentration h. The chemical repellent was placed at the center of the domain. We set $d = 0.12$ and $\gamma_3 = 200/3$.

The output obtained after the plasmodium encounters the repellent area depends on the value of h. As expected, when h is sufficiently small, the migration speed does not decrease and the leading edge progresses through the area containing the repellent. In contrast, the localized concentration pattern of solation factors disappears for large h and the organism stops migrating. The refractory state is not a final state due to the conserved mass $(s + w)$. The system described by (14) can be reactivated at locations other than the area containing the repellent, and the organism begins to move again. However, the position of the frontal edge, which is reformed after disappearing, and the migration direction both change depending on h. Three different types of output are qualitatively observed as h is increased.

For $h = 0.04$, after the leading edge touches the area containing the repellent, the activity of the system described by (14) gradually decreases and the leading edge stops migrating near the repellent area [Fig. 8(a)]. In this case, a small quantity of sol and gel can overcome the effect of the repellent area; the activity of the system then recovers on the right-hand side of the repellent area and the localized concentration structure of solation factors is created again on the right-hand side of the organism. As a result, the propagation direction is preserved, which corresponds to penetration behavior [Fig. 3(a)].

For $h = 0.07$, the leading edge cannot pass through the repellent area and the leading edge stops migrating [Fig. 8(c)]. In this case, the activity of the system described by (14) cannot recover on the right-hand side of the organism, which implies that further migration to the right-hand side of the repellent area cannot occur. When the amount of sol (s) at the rear edge recovers, the activity of the system once again increases on the left-hand side of the repellent area and a localized concentration pattern of solation factors is newly created near the rear edge. This localized pattern then propagates to the left; that is, rebound behavior is observed.

When an intermediate value of h is taken ($h = 0.05$), both types of dynamics are observed. The system described by (14) is activated at both edges after the organism encounters the chemical repellent. The organism is then divided into two bodies; that is, splitting behavior is observed [Fig. 8(b)].

In our numerical simulations, we find that migration occurs when a localized pattern of v appears at the leading edge. This localized pattern can appear when a sufficient quantity of s is present. The transition between the refractory and activated states of the leading edge that takes place during avoidance of the toxic region is due to the saddle structure of the kinetics part of (14). That is, the on-off switching of chemical reactivity is sensitive to s at the locations where a new leading edge appears.

V. DISCUSSION

We have found numerically that the transient dynamics between the active locomotion and quiescent states, as observed experimentally (Fig. 3), can be described as transient dynamics between the activated and refractory states of the autocatalytic chemical reaction taking place in the gel layer. Such transient dynamics is not sensitive to the choice of parameters in the kinetics parts of (14). However, the three experimentally observed types of transient dynamics (penetration, rebound, and splitting) can be reproduced when other parameters such as k_1, which control the activity of the autocatalytic reaction, are used as control parameters instead of r_v.

It has been reported that the three types of output shown in Fig. 8 can be observed in some activator-substrate-type reaction-diffusion systems. A typical example is the Gray-Scott model [2,22]. However, the on-off switching of chemical reactivity cannot be observed in either the Gray-Scott model or our conventional model proposed in Ref. [2]. Because no interaction is assumed between the chemical reactions that generate the leading edge and the protoplasmic sol in the conventional model, the regeneration of the localized concentration pattern shown in Fig. 3 is not observed; the solution converges to the trivial background state once the localized pattern has disappeared. In our new model, this regeneration process was successfully reproduced by incorporating interaction between the system described by (14) and the protoplasmic sol.

We have represented the autocatalytic chemical reaction that regulates the stiffness of the frontal part of the organism by a simple reaction-diffusion system. It is plausible that the chemical reaction controlling the gel stiffness can be represented by a localized pulse in the reaction-diffusion system because, as reported in Refs. [10–15], the concentrations of some chemicals such as Fragmin, Ca^{2+}, and ATP have been found to be locally high at leading edges. Furthermore, it has been experimentally observed that migration only occurs when the localized concentration pattern is present [23]. These experimental results suggest that the interaction between the two types of dynamics, that is, the protoplasmic streaming of the sol and the chemical reaction that takes place at the leading edge, is critical for maintaining the migration process. This is supported by the observation that, as shown in Fig. 7(b), when the quantity of sol at the leading edge is decreased by amputation of the main body, migration stops after a finite distance. An appropriate coupling of these two effects is thus necessary to reproduce the experimentally observed locomotion.

The contemplative behavior found in *Physarum* might be generalized to the behavior of higher animals. Cognitive behavior in humans is found within a given context. A typical example may be found in Shakespeare's tragedy "Hamlet." When Hamlet encounters a psychological problem (doubt as to whether or not his uncle, the present king, assassinated his father, the former king), he delays taking clear action for a long time because he cannot decide on a suitable course of action. However, Hamlet suddenly acts after choosing his path. Activity in the quiescent state (state of inaction) contrasts strongly with vigorous action, and the duration of the quiescent state differs from case to case and is difficult to predict. This parallels the contemplative behavior observed in *Physarum*. Insofar as the behavior of an organism represents the final output of information processing, the analysis of complex behavior can provide a basis for considering the common characteristics of living systems over a wide area of the evolutionary phylogenetic tree.

ACKNOWLEDGMENTS

This work was supported by a Grant-in-Aid for Young Scientists (B) 20740055, a Grant-in-Aid for Scientific Research (B) 21340019, Grant-in-Aid for Scientific Research on Innovative Areas 211200001, the Japan Society for the Promotion of Science (JSPS) KAKENHI 20300105, a Grant-in-Aid, and by the Human Frontier Science Program RGP51/2007.

[1] D. Bray, *Wetware—A Computer in Every Living Cell* (Yale University Press, New Haven & London, 2009).
[2] S. Takagi, Y. Nishiura, T. Nakagaki, T. Ueda, and K. I. Ueda, *Proceedings of the International Symposium On Topological Aspects of Critical Systems and Networks* (World Scientific, Singapore, 2007), p. 86.
[3] Y. Nishiura, T. Teramoto, and K. I. Ueda, Phys. Rev. E **67**, 056210 (2003).
[4] Y. Nishiura, T. Teramoto, and K. I. Ueda, Chaos **13**, 962 (2003).
[5] T. Teramoto, K. I. Ueda, and Y. Nishiura, Phys. Rev. E **69**, 056224 (2004).
[6] Y. Nishiura, T. Teramoto, and K. I. Ueda, Chaos **15**, 047509 (2005).
[7] A. Tero, R. Kobayashi, and T. Nakagaki, Physica D **205**, 125 (2005).
[8] R. Kobayashi, A. Tero, and T. Nakagaki, J. Math. Biol. **53**, 273 (2006).
[9] V. A. Teplov, Yu. M. Romanovsky, and O. A. Latushkin, BioSystems **24**, 269 (1991).
[10] T. Ueda, K. Matsumoto, T. Akitaya, and Y. Kobatake, Exp. Cell Res. **162**, 486 (1986).
[11] T. Ueda, T. Nakagaki, and T. Yamada, J. Cell. Biol. **110**, 1097 (1990).
[12] K. Natsume, Y. Miyake, M. Yano, and H. Shimizu, Cell Struct. Func. **18**, 111 (1993).
[13] K. Natsume, Y. Miyake, M. Yano, and H. Shimizu, Protoplasma **166**, 55 (1992).
[14] T. Hasegawa, S. Takahashi, H. Hayashi, and S. Hatano, Biochemistry **19**, 2677 (1980).
[15] D. T'Jampens, K. Meerschaert, B. Constantin, J. Bailey, L. J. Cook, V. de Corte, H. de Mol, M. Goethals, J. van Damme, J. Vanderkerckhove, and J. Gettemans, J. Cell Sci. **110**, 1215 (1997).
[16] T. Q. P. Uyeda, S. Hatano, and M. Furuya, Cell Motil. Cytoskeleton **10**, 410 (2005).
[17] S. Yoshiyama, M. Ishigami, A. Nakamura, and K. Kohama, Cell Biol. Int. **34**(1), 35 (2010).

[18] T. Ueda, T. Nakagaki, and Y. Kobatake, Protoplasma Suppl. **1**, 51 (1988).

[19] Y. Yoshimoto, T. Sasaki, and N. Kamiya, Protoplasma **109**, 159 (1981).

[20] Y. Yoshimoto, F. Matsumura, and N. Kamiya, Cell Motil. **1**, 433 (1981).

[21] H. Sesaki and S. Ogihara, J. Cell Sci. **110**, 809 (1997).

[22] Y. Nishiura, Y. Oyama, and K. I. Ueda, Hokkaido Math. J. **36**(1), 207 (2007).

[23] Y. Mori, K. Matsumoto, T. Ueda, and Y. Kobatake, Protoplasma **135**, 31 (1986).